

UNCLASSIFIED

Defense Technical Information Center  
Compilation Part Notice

ADP012633

TITLE: Optical Characterization of IV-VI Mid-Infrared VCSEL

DISTRIBUTION: Approved for public release, distribution unlimited

This paper is part of the following report:

TITLE: Progress in Semiconductor Materials for Optoelectronic Applications Symposium held in Boston, Massachusetts on November 26-29, 2001.

To order the complete compilation report, use: ADA405047

The component part is provided here to allow users access to individually authored sections of proceedings, annals, symposia, etc. However, the component should be considered within the context of the overall compilation report and not as a stand-alone technical report.

The following component part numbers comprise the compilation report:  
ADP012585 thru ADP012685

UNCLASSIFIED

## OPTICAL CHARACTERIZATION OF IV-VI MID-INFRARED VCSEL

F. Zhao, H. Wu, T. Zheng, P. J. McCann, A. Majumdar, Lalith Jayasinghe and Z. Shi  
School of Electrical and computer Engineering  
202 West Boyd, University of Oklahoma, Norman, OK 73019

### ABSTRACT

PbSe/PbSrSe multiple-quantum-well (MQW) structures and PbSrSe thin films were grown on BaF<sub>2</sub> (111) substrates by molecular beam epitaxy (MBE) and characterized by Fourier transform infrared (FTIR) spectrometer. Strong photoluminescence without Fabry-Perot interference fringes was observed even at room temperature from the MQW structures. The peak energies for the MQW structures with different well widths shifted to high energy with increasing temperature. The absorption edge of PbSrSe layer was determined by transmission spectra. Meanwhile, we designed and fabricated  $\lambda=4.1\ \mu\text{m}$  MQW vertical cavity surface emitting laser (VCSEL). A power output of 40 mW was obtained at room temperature. The room temperature threshold pump density is  $200\ \text{kW/cm}^2$ .

### INTRODUCTION

Mid-infrared diode lasers are mainly used for trace-gas-sensing applications [1]. This is due to the fact that the numerous absorption lines of many gaseous molecules, such as CO<sub>2</sub>, CH<sub>4</sub>, N<sub>2</sub>O, HCl, etc., are in the range of mid-infrared spectra. Performance requirements that are not yet available include continuous wave (cw) operation at thermoelectric cooler range ( $T \geq 240\ \text{K}$ ), spectral purity, and reasonable output powers ( $\geq 1\ \text{mW}$ ) with good beam quality. Although substantial advances have been made in the development of edge emitting mid-infrared diode lasers, including IV-VI lead-salt [2], quantum cascade (QC) [3,4] and type-II quantum well (QW) devices [5], there has little progress until recently in developing mid-IR vertical cavity surface emitting laser (VCSEL). This is despite the attractive performances of VCSELs, such as low-divergence circular beams, single mode operation, and the high possibility of two-dimensional monolithic integration arrays.

It is well known that the presence of the Auger recombination in narrow gap semiconductors is the major factor limiting high temperature operation of mid-infrared lasers. The major advantage of lead salt materials is that the Auger coefficients are more than one or two orders of magnitude lower than other mid-IR materials with a comparable bandgap [6,7], and it will not prevent quantum structure of these materials from achieving room temperature laser operation [6]. We proposed and demonstrated the first IV-VI VCSEL on BaF<sub>2</sub> (111) substrate [8]. Such VCSELs have obtained near-room-temperature pulsed operation 300mW output power [9,10] and threshold density as low as  $10.5\ \text{kW/cm}^2$  [11]. In this paper, we report optical characterization of IV-VI PbSe/PbSrSe MQW structures and PbSrSe layer for VCSEL. The optical properties of the VCSEL are also given.

## EXPERIMENTAL DETAIL

The PbSe/PbSrSe MQW structures and PbSrSe thin films were grown on BaF<sub>2</sub> (111) substrates by molecular-beam epitaxy (MBE) in an Intevac Modular Gen II system using compound sources for PbSe and BaF<sub>2</sub>, and elemental sources for Sr and Se. The three MQW structures grown are with well layer thickness of 10, 16, 20 nm and with barrier layer thickness of 30, 40, 37 nm, respectively. A Sr-to-PbSe flux ratio of 3% was used to grow the PbSrSe barriers in PbSe/PbSrSe MQW structures. The Pb<sub>1-x</sub>Sr<sub>x</sub>Se thin film was grown with Sr-to-PbSe flux ratio from 3% up to 100%. Based on the results obtained from the samples mentioned above, we designed and grew a VCSEL structure in this MBE system. The typical structure is plotted in Fig. 1. The VCSEL structure mainly consists of a bottom mirror, a PbSe/PbSrSe MQW active layer and a top mirror. The bottom and top mirrors were fabricated with 3-pair quarter-wave stack of Pb<sub>0.97</sub>Sr<sub>0.03</sub>Se (188 nm)/BaF<sub>2</sub> (591 nm) and Pb<sub>0.75</sub>Sr<sub>0.35</sub>Se (282 nm)/BaF<sub>2</sub> (599 nm), respectively. The active layer consists of a  $\lambda/2$ -cavity of 9-period PbSe (20 nm)/Pb<sub>0.97</sub>Sr<sub>0.03</sub>Se (20 nm) multiple QW structure. Details of the growth techniques for PbSe/PbSrSe MQW VCSEL have been published elsewhere [12]. Large difference of reflective indices between the Pb<sub>0.97</sub>Sr<sub>0.03</sub>Se ( $n \sim 4.7$ ) and BaF<sub>2</sub> ( $n=1.46$ ) yields more than 99% high reflectivity with only a three-pair stack for the bottom mirror. The higher strontium content of 35% is used to fabricate the top mirror for the first time so that the absorption edge of Pb<sub>0.75</sub>Sr<sub>0.35</sub>Se is beyond 1.064  $\mu$ m pump source. The absorption edge was determined by the transmission measurement.

The samples were characterized by the photoluminescence (PL), transmission and reflection measurements with the aid of the BRUKER IFS 66/S Fourier transform infrared (FTIR) spectrometer. Without further processing, the samples were mounted on a copper holder within a cryostat and illuminated with a 1.064  $\mu$ m Nd:YAG laser ( $\tau_{\text{pulse}} \approx 50$  ns, 10 Hz) at an incident angle of 75° for PL and laser emission measurement. The standard synchronal output signal was used as trigger source during measurement. The spot size focused on the sample surface was 4 mm $\times$ 6 mm for PL measurement. The signals coming from the samples was collected by two planar mirrors and two concave mirrors, passed through 2.47  $\mu$ m long-pass filter to cut off the signal of the pump beam and measured by the IFS 66/S spectrometer. A polarizer controlled the pump intensity by changing the angle of the polarizer, and an LN<sub>2</sub>-cooled InSb detector with a 6  $\mu$ m cutoff wavelength detected the emission radiation. The pump power density for the PL measurement is kept about 200 kW/cm<sup>2</sup>. The temperature range of the measurements is 80-300 K.

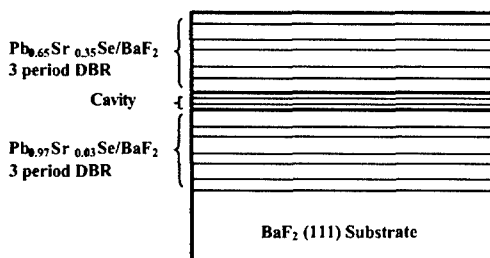


Figure 1. VCSEL structure schematic.

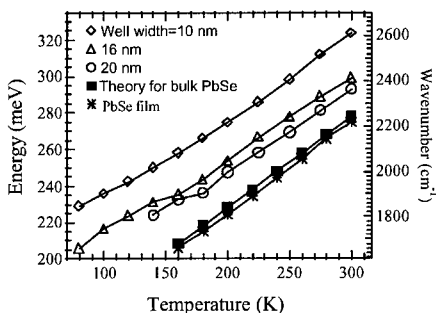
## RESULTS AND DISCUSSION

Fig. 2 displays the temperature dependence of PL peak energies for the three MQW samples with different well layer thicknesses. Also shown is the PL energy change for the PbSe thin film grown on the (111) BaF<sub>2</sub> substrate. The PL peak energies increase monotonously with temperature from 80 to 300 K and decrease with the increase of the well layer thicknesses at the same temperature, which is attributed to recombination of quantum confined electron-hole pairs. The temperature coefficient is 0.43, 0.42 and 0.43 meV/K for 10, 16 and 20 nm well width, respectively. The peak energy change of bulk PbSe with temperature can be expressed theoretically as [13,14],

$$E_{g, \text{PbSe}}(\text{meV}) = 125 + (400 + 0.256T^2)^{1/2} \quad (1)$$

Where  $E_{g, \text{PbSe}}$  is bandgap energy, and  $T$  is temperature. As shown in Fig. 2, the theoretical value (shown as solid square in Fig. 2) is good agreement with the experiment data (0.498 meV/K). To optimize the VCSEL performance at a certain temperature, one needs to align the gain peak to the cavity resonance. The results above-mentioned are favorable to design and fabricate high performance VCSEL.

The measured PL spectra at 160 K and room temperature from the three MQW structures with different well layer thickness are shown in Fig. 3 (a) and (b), respectively. The spectra were collected with a resolution of 8 cm<sup>-1</sup> (1 meV) and a coaddition of 128 times. To be able to compare the PL intensities of single QW between the three samples, we divided the measured PL intensities by the corresponding QW period number in the sample. As the well layer thickness decreases, the peak energies shift towards higher energies (blueshift). At low temperature, the full width at half maximum (FWHM) decreases from 8.2 to 7.2 meV as the well layer thickness is decreased from 20 to 10 nm. However, such change of FWHM is not observed at room temperature spectra. The PL intensity is increased with decreasing well layer thicknesses and up to maximum for 10 nm well width.



**Figure 2.** The PL peak energies as a function of temperature. The well width is 10 nm (diamond), 16 nm (triangle) and 20 nm (circle), respectively. The solid square and star show the calculation values from equation (1) and measured values from bulk PbSe, respectively.

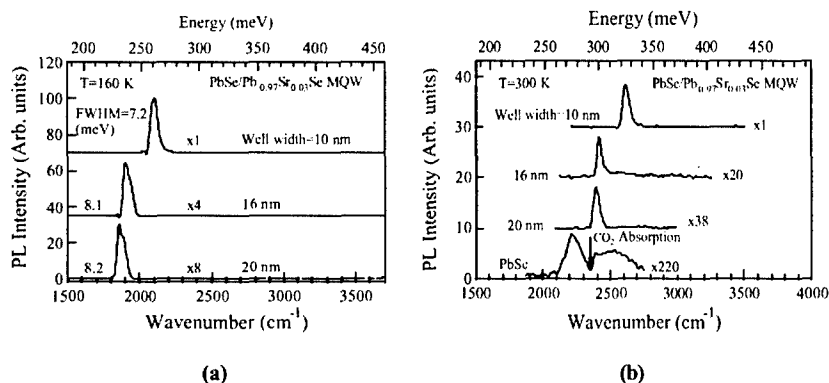


Figure 3. PL spectra for different well widths at (a) 160 K and (b) room temperature.

In comparison, the PL spectrum for PbSe thin film with thickness of 2  $\mu\text{m}$  is also shown in Fig. 3 (b). The broad FWHM can be clearly observed. Note that the spectrum for bulk PbSe around 2400  $\text{cm}^{-1}$  is distorted due to the absorption by atmospheric  $\text{CO}_2$  in the open emission part. No interference fringes were observed for these QW samples. Normally, due to the large difference of refractive indices between the IV-VI QW layer ( $n \sim 4.7$ ) and the  $\text{BaF}_2$  substrate ( $n=1.46$ ), photoluminescence (PL) signals were often merged with the interference fringes of the layer [15], which makes it very difficult to determine the net gain peak. With the aid of short pulse Nd-YAG laser at 1.06  $\mu\text{m}$  being used as a pump source, the net gain peak is successfully confirmed. The strong PL signals obtained clearly showed amplified spontaneous emission (ASE) that significantly suppressed the interference fringes. The ASE at room temperature suggests that the Auger recombination does not limit IV-VI lasers operating above room temperature.

Increasing Sr content during  $\text{Pb}_{1-x}\text{Sr}_x\text{Se}$  growth results in the increase of the band gap. The band gap can be obtained from the measured transmission spectra for various Sr content, shown in Fig. 4. For different pump lasers, the suitable Sr content during growth of top mirror needs

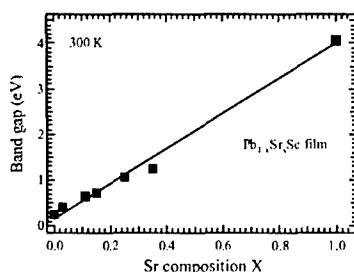
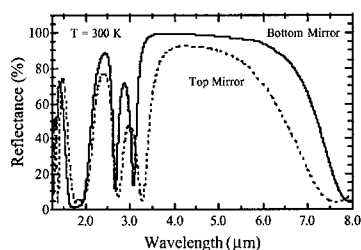


Figure 4. Band gap dependence of Sr composition.



**Figure 5.** Room temperature reflection spectra for top mirror and bottom mirror, respectively.

to be considered so that it is transparent to pump laser. For example, if the  $2.1\ \mu\text{m}$  (band gap  $\sim 0.59\ \text{eV}$ ) pump laser is used as a pump source, more than 10% Sr content (Sr-to-PbSr flux ratio) for top mirror is required. For  $1.064\ \mu\text{m}$  (band gap  $\sim 1.165\ \text{eV}$ ) Nd:YAG pump laser, the Sr content in the top mirror has to be beyond 30% so as to be with high pump efficiency.

Based on the results above-mentioned, we designed and fabricated a VCSEL device. Fig. 5 shows the reflection spectra of the top mirror and bottom mirror for the VCSEL at room temperature. The 35% Sr content was chosen to grow the top mirror so that the top mirror is basically transparent to the  $1.064\ \mu\text{m}$  pump source, as shown in Fig. 6. However, the high Sr content results in inferior top mirror, and low reflectivity of 92%. The 9 period  $\text{PbSe/Pb}_{0.97}\text{Sr}_{0.03}\text{Se}$  (20 nm/20 nm) is used as active layer. The resonance peak measured at room temperature from the reflectance of the VCSEL is well matched with the MQW gain peak of the active layer, as indicated in Fig. 6. As a result, a room temperature laser emission for the  $\text{PbSe/Pb}_{0.97}\text{Sr}_{0.03}\text{Se}$  VCSEL is obtained for the first time. Fig. 7 shows light-light emission curves measured at temperatures from 290 to 310 K. As shown in Fig. 7, above-room-temperature laser emissions were clearly observed. The maximum output power of 40 mW was obtained at room

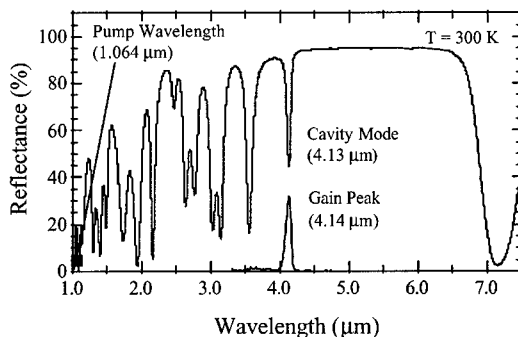


**Figure 6.** Room temperature reflection spectrum for the VCSEL shown in Fig. 1. Also shown is the gain peak on the bottom from PL measurement.

temperature. The room temperature threshold pump intensity is  $200 \text{ kW/cm}^2$ . The detailed results about the VCSEL will be published elsewhere [16].

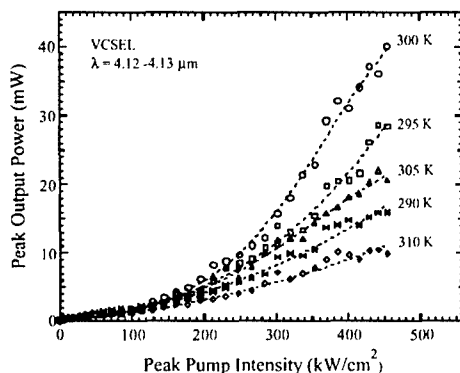


**Figure 7.** Peak VCSEL output power vs peak pump intensity at five temperatures, for a  $1.5 \text{ mm} \times 1.5 \text{ mm}$  pump spot.

## SUMMARY

The photoluminescence of PbSe/PbSrSe MQW structures grown on (111)  $\text{BaF}_2$  substrates by MBE was measured with the IFS 66/S FTIR spectrometer. A short pulse Nd:YAG laser with the wavelength of  $1.064 \mu\text{m}$  was used as pump source. The strong ASE suppressed the Fabry-Perot interference fringes so that the net gain peak was easily obtained. Through the absorption edge measurements of PbSrSe thin films determined from the transmission spectra, a high Sr content of 35% was chosen to grow the top mirror for the VCSEL fabrication. The gain peak of the VCSEL designed and fabricated was well matched with the resonance cavity mode at room temperature. As a result, we have realized the room temperature laser emission of the IV-VI PbSe/PbSrSe MQW VCSEL for the first time. The maximum peak power output is 40 mW, which does not show saturation. The room temperature threshold pump intensity is  $200 \text{ kW/cm}^2$ . The improvements in the crystal quality of the top mirror are required. A cw laser emission will be predicted as some suitable post-processes are applied for the VCSEL fabrication.

## ACKNOWLEDGEMENTS

This work was supported by DoD AFOSR, ONR, and NSF under award numbers F49620-00-1-0291, DEPSCoR N00014-00-1-0506, and ECS-0080783, respectively.

## REFERENCES

1. M. Tacke, *Infrared Phys. Technol.* **36**, 447 (1995).
2. G. Bauer, M. Kriechbaum, Z. Shi, and M. Tacke, *J. Nonlinear Opt. Phys. Mater.* **4**, 283 (1995).
3. S. Slivken, A. Matlis, A. Rybaltowski, Z. Xu, and M. Razeghi, *Appl. Phys. Lett.* **74**, 2758 (1999).
4. A. Tahraoui et al., *Appl. Phys. Lett.* **78**, 416 (2001).
5. W. W. Bewey, C. L. Felix, I. Vurgaftman, D. W. Stokes, E. H. Aifer, L. J. Olafsen, J. R. Meyer, M. J. Yang, B. V. Shanabrook, H. Lee, R. U. Martinelli, and A. R. Sugg, *Appl. Phys. Lett.* **74**, 1075 (1999).
6. R. Klann, T. Hofer, R. Buhleier, T. Elsaesser, and J. W. Tomm, *J. Appl. Phys.* **77**, 277 (1995).
7. P. C Findlay, C R Pidgeon, B N Murdin, A F G van der Meer, A F G Langerak, C M Ciesla, J Oswald, G Springholz and G Bauer, *Phys. Rev. B* **58**, 12908 (1998).
8. Z. Shi, G. Xu, P.J. McCann, and X. M. Fang, N. Dai, C. L. Felix, W. W. Bewley, I. Vurgaftman, and J. R. Meyer, *MRS 1999 Fall meeting*, Nov. 30, 1999, Boston Massachusetts.
9. Z. Shi, G. Xu, P. J. McCann, X. M. Fang, N. Dai, C. L. Felix, W. W. Bewley, I. Vurgaftman, and J. R. Meyer, *Appl. Phys. Lett.* **76**, 3688 (2000).
10. W. W. Bewley, C. L. Felix, I. Vurgaftman, J. R. Meyer, G. Xu, and Z. Shi, *Electron. Lett.* **36**, 539 (2000).
11. C. L. Felix, W. W. Bewley, I. Vurgaftman, J. R. Lindle, J. R. Meyer, H. Z. Wu, G. Xu, S. Khosravani, and Z. Shi, *Appl. Phys. Lett.* **78**, 3770 (2001).
12. H. Wu, F. Zhao and Z. Shi, *20<sup>th</sup> North American Conference on Molecular Beam Epitaxy*, Oct. 1-3, 2001, Providence, Rhode Island.
13. U. Schiessl and J. Rohr, *Infrared Technol.* **40**, 325 (1999).
14. G. Springholz, T. Schwarzl, W. Heiss, G. Bauer, M. Aigle, H. ASCHER, I. Vavra, *Appl. Phys. Lett.* **79**, 1225 (2001).
15. P. J. McCann, K. Namjou, and X. M. Fang, *Appl. Phys. Lett.* **75**, 3608 (1999)
16. F. Zhao, H. Wu, Lalith Jayasinghe and Z. Shi, accepted and to be published in *Appl. Phys. Lett.*, in Feb. 2002.